

# Sintering behaviour of gel-derived powders

L. MONTANARO, A. NEGRO

*Dipartimento di Scienza dei Materiali e Ingegneria Chimica, Politecnico, Corso Duca Degli Abruzzi 24, 10129 Torino, Italy*

85Al<sub>2</sub>O<sub>3</sub>–15ZrO<sub>2</sub> (wt %) powders were synthesized by gel precipitation starting from AlCl<sub>3</sub>·6H<sub>2</sub>O and ZrCl<sub>4</sub> solutions and dried by two different methods: (i) by spray-drying and (ii) via a sol–gel route by n-octanol in a pilot plant. The particles by process (i) were spherical granules of diameter 15 μm, and those by process (ii) were microspheres of 25 μm. The powders were characterized in terms of morphology, particle size distribution, surface area, weight loss and crystallization behaviour at different temperatures. Shrinkage, microstructure, density and pore size distribution were evaluated on compacts at different temperatures to study the sintering kinetics. Experimental observations suggest that (a) the use of controlled-geometry powders allows one to obtain high green densities; and (b) the sintering of gel-derived powders develops in two steps: during the first one, sintering mainly takes place inside each microsphere (or granule), and during the second step, mainly between the microspheres (or granules). At temperatures > 1100 °C, sintering produces shrinkage of the microspheres (or granules) leading to pore formation between them, which prevents the achievement of high densities. Only by using hot pressing is it possible to obtain theoretical densities and high mechanical properties.

## 1. Introduction

Barringer *et al.* [1] suggest that the major contributor to the cost of rejection is that current processing methods using conventional ceramic powders produce green bodies that are inhomogeneously packed; it is consequently difficult to control the sintering process. Bruch [2] showed that the particle arrangement strongly affects sintering kinetics and, according to Lange [3], “particle arrangement, a parameter neglected by theorists and many experimentalists, significantly influences sinterability”.

The purpose of this paper is (a) the production, by two different processes via gel, of Al<sub>2</sub>O<sub>3</sub>–ZrO<sub>2</sub> powders having controlled chemistry and geometry to make a green microstructure with a uniform distribution of pores and as many particle–particle contacts as possible; and (b) an evaluation of the influence of the production process on the characteristics of the powders and on their sintering.

## 2. Experimental procedure

### 2.1. Powder preparation

To produce alumina–zirconia composites containing 15 wt % ZrO<sub>2</sub>, suitable quantities of AlCl<sub>3</sub>·6H<sub>2</sub>O and ZrCl<sub>4</sub> were dissolved in distilled water. The hydroxides were precipitated at 25 °C by adding 4N NH<sub>4</sub>OH under continuous stirring; the ultimate pH of 9 was chosen by zeta-potential measurements.

The gel was washed several times to remove precipitation by-products, particularly Cl<sup>−</sup> ions; the final Cl<sup>−</sup> ion content was 0.4 mol Cl<sup>−</sup> per mol Al<sup>3+</sup>. Small amounts of gibbsite and bayerite were identified by X-ray diffraction (XRD) and by thermogravimetric

analysis (TG–DTG) on the washed gel dried at 105 °C [4].

The gel was divided into two parts: the first one was dried at 300 °C by spray-drying (this powder will be called SD); the second part was peptized by HCl in a sealed vessel at 80 °C for 48 h. The resulting sol was concentrated at 80 °C under stirring to reach an Al<sup>3+</sup> ion content of about 2 mol l<sup>−1</sup>.

During the concentration step, using laser granulometry it was verified that agglomeration had not taken place. The sol was introduced through a small nozzle and broken up in droplets which slowly dehydrated from contact with 1-octanol and converted into solid gel microspheres. The pilot plant for production of microspheres has been described elsewhere [5, 6]. The microspheres drawn from the pilot plant were dried at 300 °C. This powder will be called MS.

### 2.2. Powder characterization

The microstructure, particle size, surface area and phases were studied by the following techniques: scanning electron microscopy (SEM), laser granulometry, BET, and XRD at different temperatures.

### 2.3. Powder sinterability

The SD and MS powders were heated at 1200 °C for 30 min; this thermal treatment was done according to previous experiments carried out on alumina–zirconia composites obtained via a gel [7].

For dilatometric measurements and sinterability tests, samples of 3 mm × 3 mm × 25 mm were made with the SD and MS powders by uniaxial pressing

(200 MPa). The samples were then heated for 30 min at different temperatures (1100, 1200, 1300, 1400 and 1500 °C).

The porosity and pore size distribution of the compacts were evaluated by mercury porosimetry. The fracture surfaces and the morphology of the pellets were investigated by SEM.

### 3. Results

#### 3.1. Powder characterization

The micrographs of Fig. 1 show typical morphologies of the powders; it is possible to observe that, while the SD powder is formed by spherical granules made up of small dense agglomerates, the MS powder consists of microporous spheres.

Laser granulometry analysis showed that the particle size distribution of the MS powder is more uniform than that of the SD powder and that the average sizes of the SD and MS powders are respectively 15 and 25  $\mu\text{m}$  (Fig. 2). For both powders the ratio  $D_{\text{max}}/D_{\text{ave}}$  is lower than 3, the value characteristic of "ideal" powder [1].

The BET surface areas of the SD and MS powders are respectively 250 and 350  $\text{m}^2 \text{g}^{-1}$  after thermal treatment at 300 °C; it decreases for both powders by 18–20  $\text{m}^2 \text{g}^{-1}$  after thermal treatment at 1200 °C.

XRD patterns taken at different temperatures are presented in Fig. 3; it is possible to observe that

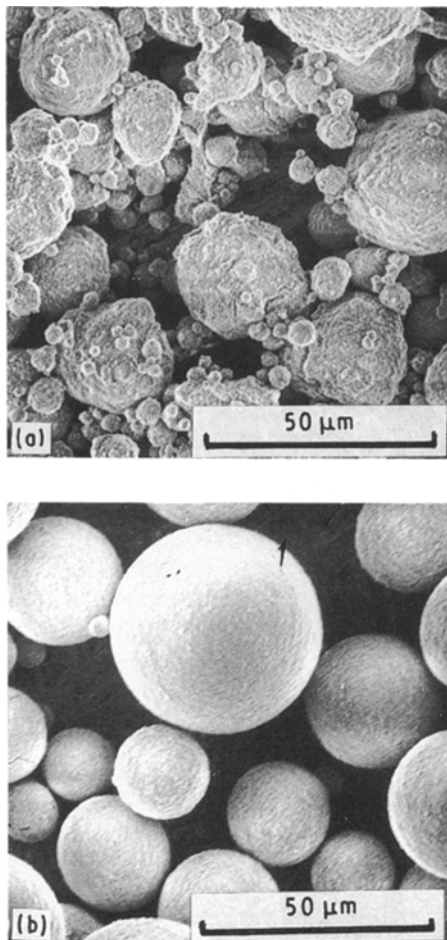


Figure 1 Morphologies of (a) SD and (b) MS powders.

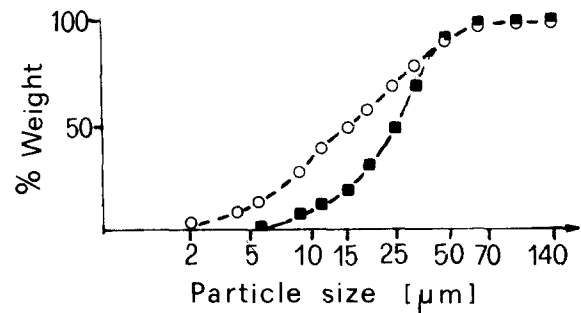


Figure 2 Particle size distribution of ( $\circ$ ) SD and ( $\blacksquare$ ) MS powders.

$\theta\text{-Al}_2\text{O}_3$  is present up to 1300 °C but, in the MS sample, its content is higher.

#### 3.2. Powder sinterability

The dilatometric curves are presented in Fig. 4: for the SD sample the shrinkage is 7.1% and it starts at 1080 °C, while for MS it is 5.2% and starts at 1015 °C. These differences are probably due to the different  $\theta\text{-Al}_2\text{O}_3$  contents and to the different powder microstructures.

Fig. 5 illustrates the bulk density versus temperature: an end-point density of 0.82  $\rho_t$  and 0.88  $\rho_t$  is achieved at 1500 °C for SD and MS samples, respectively. The green density of SD samples was 0.41  $\rho_t$  and that of the MS 0.47  $\rho_t$ ; both powders pack in a favourable way, particularly MS powder.

Mercury intrusion data are presented in Fig. 6. The total intrusion volume and average pore size of the MS samples are, at each temperature, smaller than those of the SD samples according to the bulk density measurements; furthermore, the pore size distribution of MS samples is narrower.

Between 1100 and 1400 °C the pore volume connected by the smaller capillaries decreases whereas the pore volume connected by larger capillaries increases; at higher temperatures, larger capillaries begin to disappear. This behaviour is in accordance with Lange's observations on alumina powder having a grain size < 1  $\mu\text{m}$  [3].

Fig. 7 illustrates the unpolished surface of an MS sample at room temperature. As can be seen, it is not possible to identify the microspheres. The microstructure can be described as small dense domains separated by interconnecting pores; by observation of the fracture surfaces, it is seen that the microspheres are partially intact and well packed (Fig. 8). The SD sample shows the same microstructure.

At 1100 °C the microstructure is changed: on the surface of the sample one can identify dense regions separated by elongated pores. The formation of these pores is connected with domain sintering (Fig. 9).

Up to 1300 °C the microstructure is not changed; at this temperature the sintering between domains is more evident (Fig. 10). The domains appear fully dense and support grain growth.

At 1400 °C the boundaries between microspheres are more marked (Fig. 11) and this explains the large pores emphasized by porosimetric measurements. The sintering is progressing and most domains become

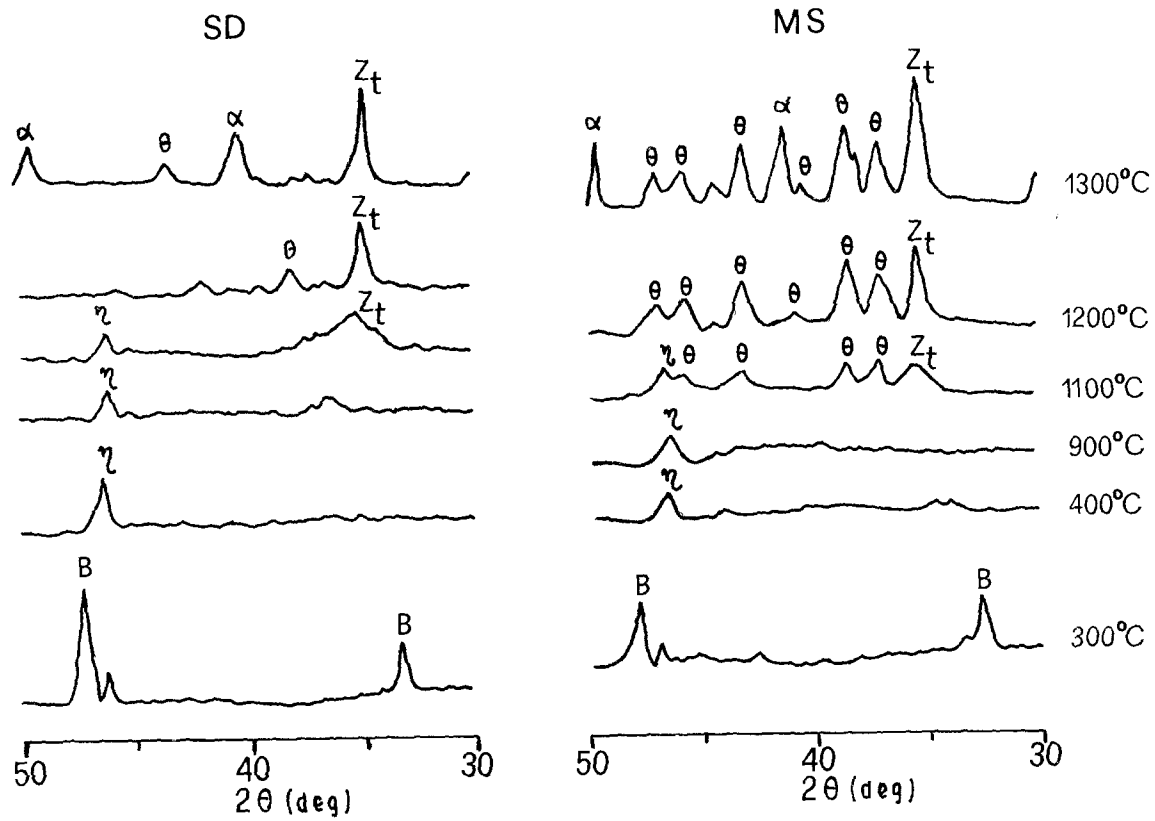


Figure 3 XRD patterns at different temperatures of SD and MS powders.

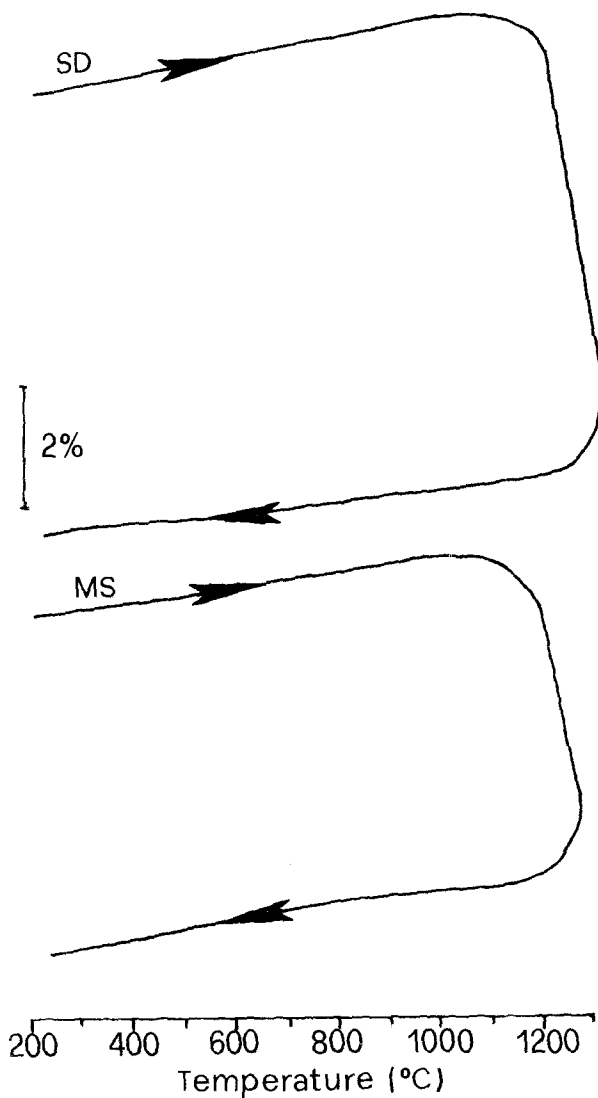


Figure 4 Dilatometric curves of SD and MS powder compacts.

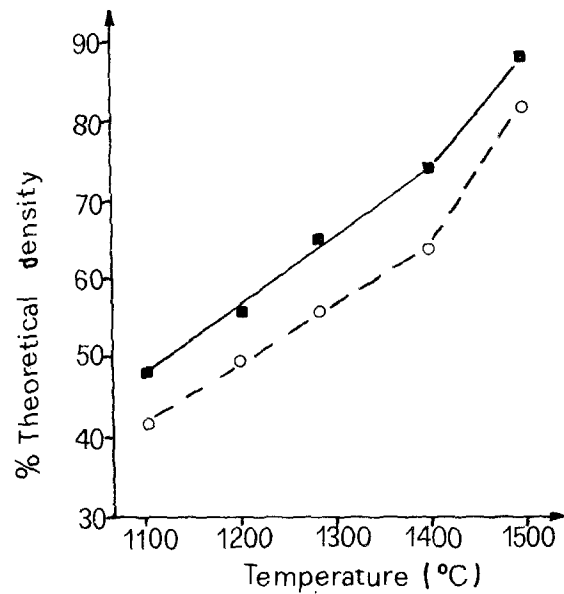


Figure 5 Bulk densities versus temperature (30 min soak) for (○) SD and (■) MS powders, cast at 200 MPa.

single grains (Fig. 12). Grain growth, which initiated within the domains, continues within dense agglomerates; grains double their size between 1300 and 1400 °C.

Fig. 13 illustrates the surface of samples treated at 1500 °C. Grain growth does not appear between 1400 and 1500 °C and the microstructure is very uniform. Some pores still exist between microspheres, as is evident from fracture surfaces examinations (Fig. 14); these pores nevertheless have a coordination number of 3, and therefore, as Kingery and Francois recognized [8], they are able to disappear on increasing the time or the temperature of sintering.

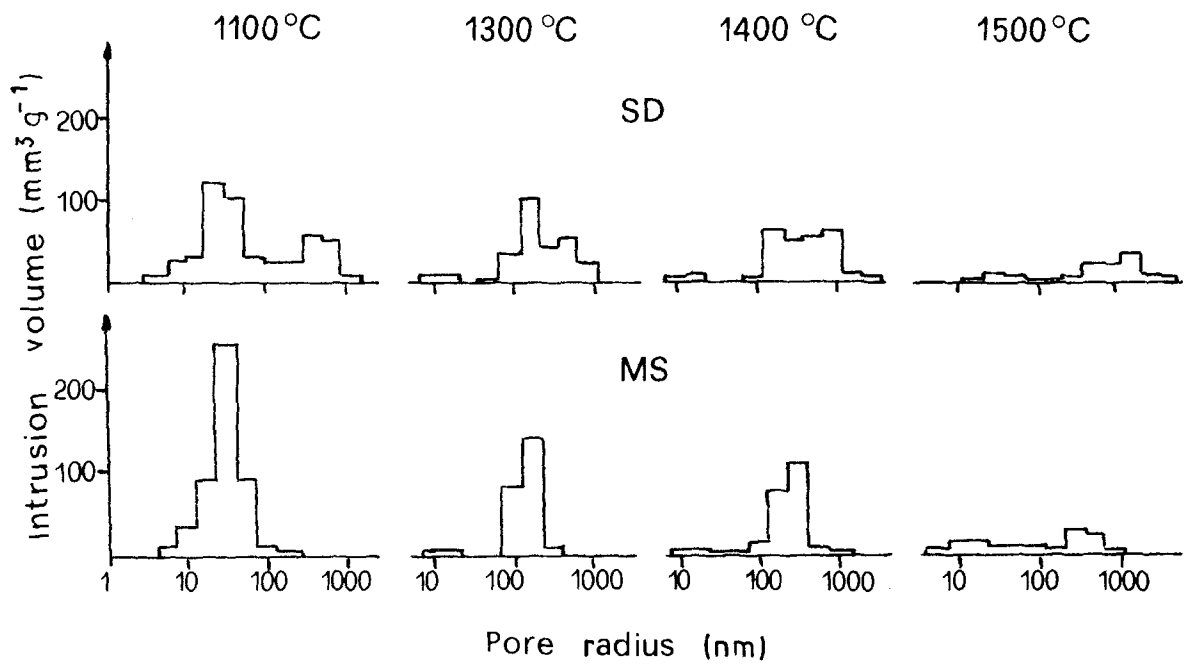


Figure 6 Volume of intruded mercury versus capillary size at different sintering temperatures (30 min soak) for SD and MS powder compacts.

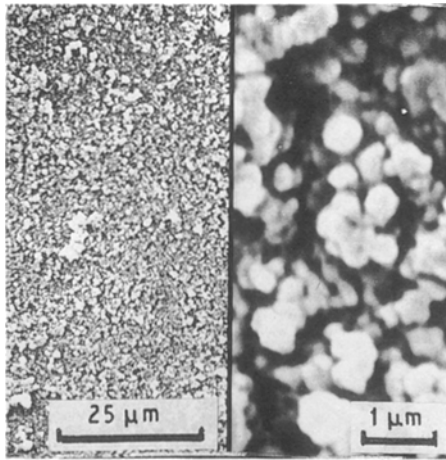


Figure 7 Microstructure of unpolished surface of MS green body cast at 200 MPa at room temperature.

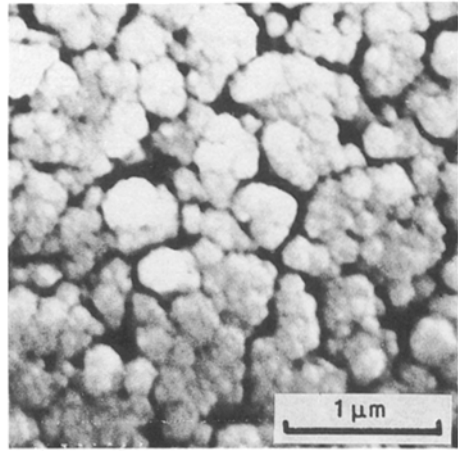


Figure 9 Microstructure of unpolished surface of MS sample cast at 200 MPa and sintered at 1100 °C for 30 min.

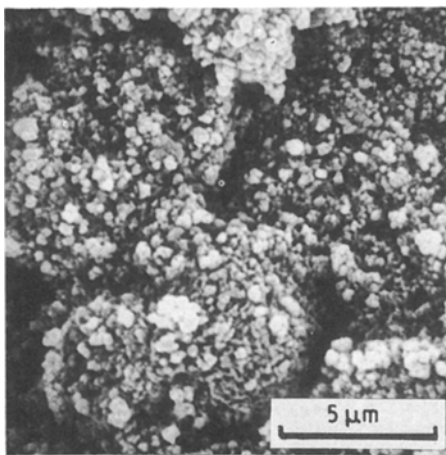


Figure 8 Fracture surface of MS green body cast at 200 MPa at room temperature.

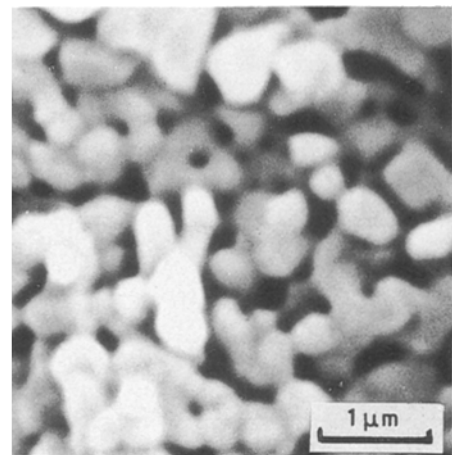


Figure 10 Microstructure of unpolished surface of MS sample cast at 200 MPa and sintered at 1300 °C for 30 min.

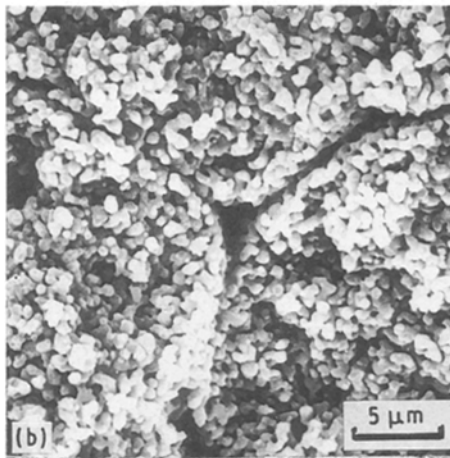
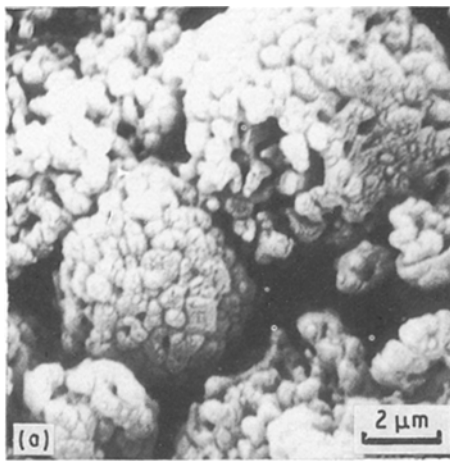


Figure 11 Fracture surface of (a) SD and (b) MS samples cast at 200 MPa and sintered at 1400 °C for 30 min.

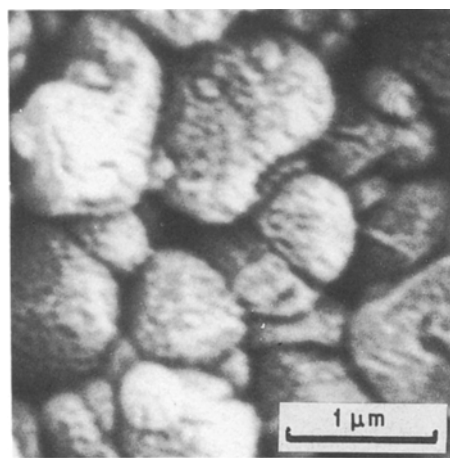


Figure 12 Microstructure of unpolished surface of MS sample cast at 200 MPa and sintered at 1400 °C for 30 min.

#### 4. Discussion

Experimental observations suggest that the use of controlled-geometry powders allows one to obtain higher green densities than those produced by current powders which are neither monodispersed nor spherical.

Using a powder particle size lower than in this work, it will probably be possible to achieve higher

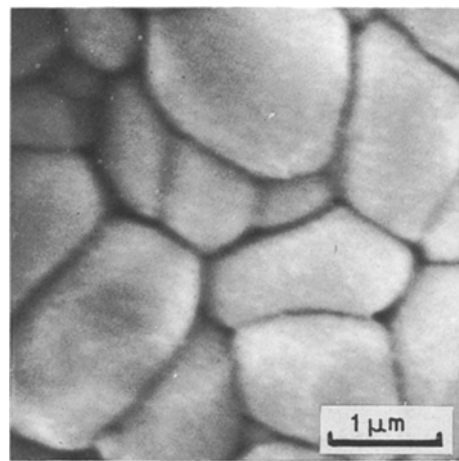


Figure 13 Microstructure of unpolished surface of MS sample cast at 200 MPa and sintered at 1500 °C for 30 min.

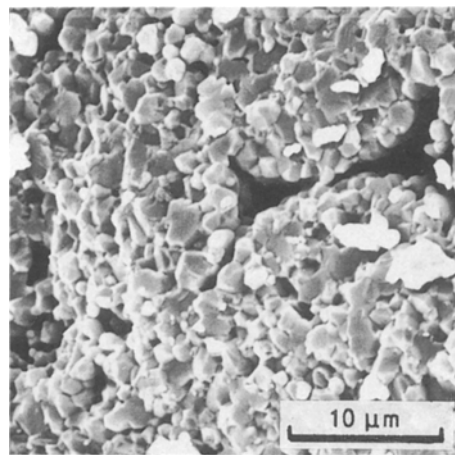


Figure 14 Fracture surface of MS sample cast at 200 MPa and sintered at 1500 °C for 30 min.

green densities as the porosity will be further reduced. These results also suggest that the sintering kinetics of the gel-derived powders formed by spherical granules (powder SD) or by microspheres (powder MS) is unlike that of the current powders.

In fact, for the powders investigated in this work, sintering develops in two steps: during the first one, sintering mainly takes place inside each microsphere (or granule); and during the second step, mainly between the microspheres (or granules).

After heat treatment at 1100 °C, the porosity of the ceramic bodies is small: in the MS samples the mean pore size is  $< 0.1 \mu\text{m}$  but sintering has just started. At 1300 °C, sintering inside the microspheres (or granules) is well advanced; the size of pores is  $< 0.5 \mu\text{m}$  and their coordination number is generally lower than 4 (Fig. 10). However, sintering produces a shrinkage of microspheres (or granules) leading to pore formation between the microspheres (or granules). Even if the coordination number of these pores is generally 3, and thus they should be able to disappear during sintering,

their size is too large to ensure high densities. In fact, as shown by the fracture surfaces, the microspheres (or granules) are only partially sintered one with another (Fig. 11).

This type of porosity is reduced but not totally removed by heat treatments at 1400 and 1500 °C. Hot pressing at 1600 °C, in contrast, gives no porous ceramic bodies with higher mechanical properties ( $\sigma_R = 735 \pm 30$  MPa;  $K_{Ic} = 10 \pm 0.5$  MPa m<sup>1/2</sup>) [9] than those obtained by Bach [7].

This means that the preliminary heat treatment of the powders at 1200 °C is effective for ceramic bodies made by hot pressing and that the strict control of powder geometry and chemistry allows one to obtain high-performance ceramics. However, in practice, hot pressing is not widely used, so to improve the conventional sintering of gel-derived powders it is necessary to modify the preliminary heat treatment. A form of heat treatment leading to a homogeneous sintering of powders and which avoids the different steps shown in this work must be found.

When this goal is achieved, it will be possible to produce alumina–zirconia composites with densities close to the theoretical value at temperatures lower than the conventional ones.

## References

1. E. BARRINGER, N. JUBB, B. FEGLEY, R. L. POBER and H. K. BOWEN, in "Ultrastructure Processing of Ceramics, Glasses and Composites", edited by L. L. Hench and D. Ulrich (Wiley, New York, 1984) Ch. 26.
2. C. A. BRUCH, *Amer. Ceram. Soc. Bull.* **41** (1962) 799.
3. F. F. LANGE, *J. Amer. Ceram. Soc.* **67** (1984) 83.
4. L. MONTANARO and B. GUILHOT, *Amer. Ceram. Soc. Bull.* **68** (1989) 1017.
5. L. MONTANARO, P. ORLANS, J. P. LECOMPTE, V. SPECCHIA, A. NEGRO and A. GIANETTO, in Proceedings of Conference on Emerging Technologies in Materials, Minneapolis, August 1987, Paper CE 1.20.
6. L. MONTANARO, in "Surfaces and Interfaces of Ceramic Materials", edited by L. C. Dufour, C. Monty and G. Petterras (Kluwer, 1989) p. 587.
7. J. P. BACH, PhD thesis, ENSM St. Etienne, France (1988).
8. W. D. KINGERY and B. FRANCOIS, in "Sintering and Related Phenomena", edited by G. C. Kuczynski, N. A. Hooton and C. F. Gibbon (Gordon & Breach, New York, 1967) p. 471.
9. L. MONTANARO, J. P. LECOMPTE, B. GUILHOT and A. NEGRO, in Proceedings of 11th Riso International Symposium, Roskilde, September 1990, edited by J. J. Bentzen, J. B. Bilde-Sørensen, N. Christiansen, A. Horsewell and B. Ralph (Risø Nat. Lab., Roskilde, 1990) p. 419.

*Received 6 August  
and accepted 20 December 1990*